

# Generation and Characterization of a Diabody Targeting the $\alpha_v\beta_6$ Integrin

Heide Kogelberg<sup>1,2</sup>, Enrique Miranda<sup>1,2</sup>, Jerome Burnet<sup>2</sup>, David Ellison<sup>2</sup>, Berend Tolner<sup>1</sup>, Julie Foster<sup>2</sup>, Carmen Picón<sup>1</sup>, Gareth J. Thomas<sup>3</sup>, Tim Meyer<sup>1</sup>, John F. Marshall<sup>4</sup>, Stephen J. Mather<sup>2</sup>, Kerry Chester<sup>1\*</sup>

**1** UCL Cancer Institute, University College London, London, United Kingdom, **2** Centre for Molecular Oncology, Barts Cancer Institute, Queen Mary University of London, John Vane Science Centre, London, United Kingdom, **3** Cancer Sciences Unit, University of Southampton, Southampton, United Kingdom, **4** Centre for Tumour Biology, Barts Cancer Institute, Queen Mary University of London, John Vane Science Centre, London, United Kingdom

## Abstract

The  $\alpha_v\beta_6$  integrin is up-regulated in cancer and wound healing but it is not generally expressed in healthy adult tissue. There is increasing evidence that it has a role in cancer progression and will be a useful target for antibody-directed cancer therapies. We report a novel recombinant diabody antibody fragment that targets specifically  $\alpha_v\beta_6$  and blocks its function. The diabody was engineered with a C-terminal hexahistidine tag (His tag), expressed in *Pichia pastoris* and purified by IMAC. Surface plasmon resonance (SPR) analysis of the purified diabody showed affinity in the nanomolar range. Pre-treatment of  $\alpha_v\beta_6$ -expressing cells with the diabody resulted in a reduction of cell migration and adhesion to LAP, demonstrating biological function-blocking activity. After radio-labeling, using the His-tag for site-specific attachment of <sup>99m</sup>Tc, the diabody retained affinity and targeted specifically to  $\alpha_v\beta_6$ -expressing tumors in mice bearing isogenic  $\alpha_v\beta_6$  +/- xenografts. Furthermore, the diabody was specifically internalized into  $\alpha_v\beta_6$ -expressing cells, indicating warhead targeting potential. Our results indicate that the new  $\alpha_v\beta_6$  diabody has a range of potential applications in imaging, function blocking or targeted delivery/internalization of therapeutic agents.

**Citation:** Kogelberg H, Miranda E, Burnet J, Ellison D, Tolner B, et al. (2013) Generation and Characterization of a Diabody Targeting the  $\alpha_v\beta_6$  Integrin. PLoS ONE 8(9): e73260. doi:10.1371/journal.pone.0073260

**Editor:** Mitchell Ho, National Cancer Institute, NIH, United States of America

**Received:** February 14, 2013; **Accepted:** July 19, 2013; **Published:** September 4, 2013

**Copyright:** © 2013 Kogelberg et al. This is an open-access article distributed under the terms of the Creative Commons Attribution License, which permits unrestricted use, distribution, and reproduction in any medium, provided the original author and source are credited.

**Funding:** This study was supported by Debbie Fund and the UCL Cancer Institute Research Trust, Cancer Research UK (grant number C34/A5149), the Department of Health and Cancer Research UK Experimental Cancer Medicine Centre (grant number C34/A7279) ([www.cancerresearchuk.org](http://www.cancerresearchuk.org)) ([www.ecmcnetwork.org.uk](http://www.ecmcnetwork.org.uk)) and the National Institute for Health Research (NIHR) Biomedical Research Centre (BRC) (ref. UCLH.BW.mn.10161 (<http://www.uclhospitals.brc.nihr.ac.uk>)). The funders had no role in study design, data collection and analysis, decision to publish, or preparation of the manuscript.

**Competing Interests:** The authors have declared that no competing interests exist.

\* E-mail: [k.chester@ucl.ac.uk](mailto:k.chester@ucl.ac.uk)

† These authors contributed equally to this work.

## Introduction

The  $\alpha_v\beta_6$  integrin is an epithelial restricted trans-membrane protein that has emerged as a promising target for antibody-directed therapies. It is up-regulated in many tumor types including pancreatic ductal adenocarcinoma, head and neck squamous cell carcinoma, ovarian cancer, colon cancer, cholangiocarcinoma and cervical cancer [1,2,3,4,5]. During embryogenesis and wound healing  $\alpha_v\beta_6$  promotes binding to extracellular matrix proteins (fibronectin, vitronectin and tenascin) facilitating cell migration [6] and activates TGF $\beta_1$  via binding to the latency associated peptide (LAP) of the TGF $\beta$  complex [7]. In cancer,  $\alpha_v\beta_6$  has been shown to modulate invasion, inhibit apoptosis and regulate expression of matrix metalloproteases (MMPs) [8]. Importantly for a cancer target,  $\alpha_v\beta_6$  is only found at very low levels in normal tissue; its expression has been reported to regulate wound healing [6] and activation of TGF $\beta_1$  in response to injury and inflammation in the lungs [9].

The various roles of  $\alpha_v\beta_6$  in cancer have not yet been fully elucidated, although it has been shown to be a contributing factor in tumor progression [4,10] and has been associated with enhanced tumorigenic properties in colon carcinoma facilitating liver metastasis [4,11], and reducing survival times in gastric carcinoma [10]. Expression of  $\alpha_v\beta_6$  has been reported during

epithelial-mesenchymal transition (EMT) and it is thought to have a role in sustaining the EMT process [12,13]. Interestingly, high levels of  $\alpha_v\beta_6$  are found in the context of K-Ras dependency in lung and pancreatic cancer cell lines [14]. Depletion of the ITGB6 gene had a clear growth inhibitory effect on these cells [15], indicating that  $\alpha_v\beta_6$  may be a tractable target in K-Ras mutant cancers. Targeting this integrin has shown tumor growth inhibition *in vivo* due to blockade of  $\alpha_v\beta_6$ -dependent activation of the TGF $\beta$  pathway [16].

Antibodies reactive specifically with  $\alpha_v\beta_6$  could have diagnostic and therapeutic utility, particularly if they have function blocking activity. Towards this, we previously engineered murine and humanized single chain Fv antibody fragments (scFvs) reactive with  $\alpha_v\beta_6$  [17]. The unique  $\alpha_v\beta_6$  specificity was gained by an insertion into the CDR3 loop of the variable heavy-chain (VH) domain of an existing scFv scaffold. Here we describe the development of an anti- $\alpha_v\beta_6$  scFv into a stable *in vivo* targeting agent in diabody format. Diabodies are non-covalently associated bivalent molecules, created from scFvs by shortening the polypeptide linker between the VH and VL domains [18]. Their bivalent nature is advantageous for targeting [19,20,21] and they provide a flexible platform for development of targeted therapeutics, particularly since their pharmacokinetics are readily modified

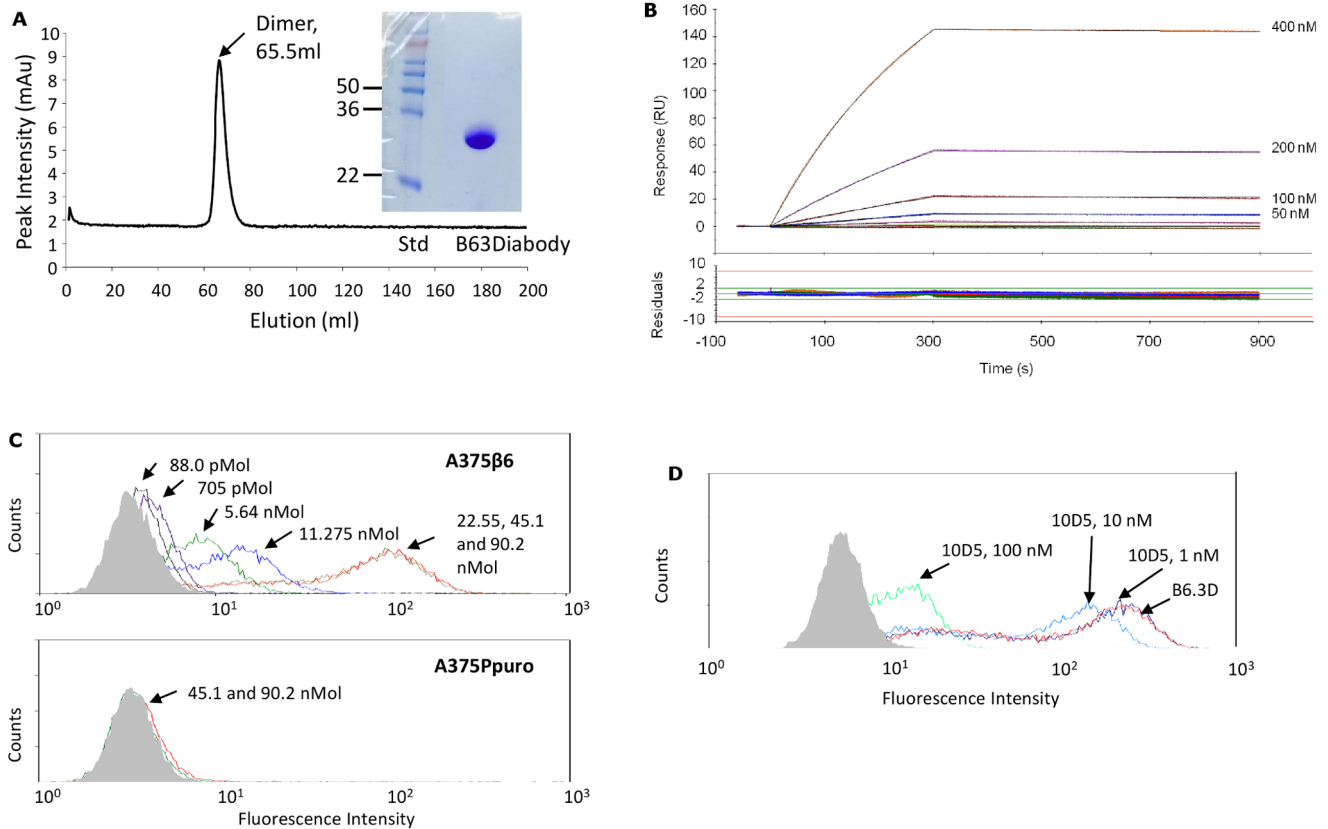


**Figure 1. Production of B6.3 diabody and analysis of its specific interaction with  $\alpha_v\beta_6$ .** A) Size-exclusion chromatographic profile (Superdex 75, 125 ml) of B6.3 diabody after fermentation, expanded-bed adsorption IMAC, Superdex 75 (500 ml), 1 ml  $\text{Ni}^{2+}$ -charged Hi-Trap IMAC, freezing and de-freezing. B6.3 diabody eluted from the column as a dimer that separated in monomeric form under reducing conditions by SDS-PAGE, consistent with non-covalent association of monomers in a diabody structure. B) Sensogram of real-time binding and dissociation of B6.3 diabody to  $\alpha_v\beta_6$ . B6.3 diabody was immobilized on a BIAcore CM5 sensor chip and  $\alpha_v\beta_6$  protein was flown across at 400, 200, 100, 50, 25, 12.5, 6.25 and 3.125 nM. The affinity constant (KD) for the interaction was  $2.8 \times 10^{-9}$  M, with on-rate of  $8,107 \pm 7.3 \text{ M}^{-1} \text{ s}^{-1}$  and off-rate of  $2.3 \times 10^{-5} \pm 1.4 \times 10^{-7} \text{ s}^{-1}$ . C) Flow cytometry analysis of B6.3 diabody binding to  $\alpha_v\beta_6$ -expressing A375P $\beta_6$  cells in a concentration-dependent manner (a) but not to A375Ppuro cells (b), which do not express this integrin. Cells were incubated with B6.3 diabody, at the indicated concentrations and binding was detected with mouse anti-tetra-histidine IgG followed by R-PE-labeled goat anti-mouse IgG. B6.3 diabody was not added to omission control (shown in solid grey). D) Inhibition of B6.3 diabody binding after incubation with the anti- $\alpha_v\beta_6$  antibody 10D5 shown by flow cytometry. Cells were incubated with 100 ng B6.3 diabody with or without prior incubation with 10D5 at the indicated concentrations. Binding of B6.3 diabody was detected with rabbit anti-hexahistidine IgG followed by R-PE-labeled goat anti-rabbit IgG. In the omission control experiment (shown in solid grey) cells were not incubated with B6.3 diabody and 10D5. doi:10.1371/journal.pone.0073260.g001

by attachment of polyethylene glycol [22]. We show that the anti- $\alpha_v\beta_6$  diabody blocks  $\alpha_v\beta_6$ -mediated biological functions. Moreover, the  $^{99\text{m}}\text{Tc}$ -labeled diabody targeted specifically to  $\alpha_v\beta_6$ +ve tumors *in vivo* within 2 hours of administration.

## Materials and Methods

### Cell lines

A375P $\beta_6$  is a  $\alpha_v\beta_6$ -positive human cell line, generated through retroviral transduction of the melanoma cell line A375P with human  $\beta_6$  cDNA and a puromycin-resistance gene as described previously [23]. The control cell line, A375Ppuro was transduced with the puromycin-resistance gene alone [23]. Both cell lines express several other RGD-binding integrins at equivalent levels, namely  $\alpha_5\beta_1$ ,  $\alpha_v\beta_3$ ,  $\alpha_v\beta_5$ ,  $\alpha_v\beta_8$  [17]. Capan-1 ( $\alpha_v\beta_6$ -positive human pancreatic cell line) was obtained from ATCC (HTB-79). All cell lines were maintained in Dulbecco's modified Eagle's medium (DMEM) (PAA Laboratories, UK) supplemented with 2 mM L-glutamine (PAA Laboratories, UK) and 10% foetal calf serum (Labtech International, Ringmer, UK).

### Production of B6.3 and shMFE23 diabody proteins

The diabody was generated from the B6.3 scFv vH and vL domains [17] by synthesizing the scFv gene with a G<sub>4</sub>S linker. The synthesized gene was obtained from Genescript (Piscataway, NJ, USA) and cloned into the pPICZ $\alpha$ BHIS vector (Invitrogen) as described previously [17]. The resulting plasmid was linearized with *Pme*I, transformed into electrocompetent *P. pastoris* X33 cells (Invitrogen) and transformants grown on YPDS and Zeocin (100  $\mu\text{g}/\text{ml}$ ; Invitrogen) plates. Positive clones were selected and screened for methanol-induced protein expression according to the manufacturer's recommendations. Clones with the highest B6.3 diabody expression were used for protein production by fermentation with initial purification using expanded-bed adsorption IMAC as previously described [24,25]. The B6.3 diabody was harvested 4 h post induction of protein expression. Final purification was performed by size-exclusion chromatography on a Superdex 75 (GE Healthcare) column (500-ml bed volume) equilibrated with phosphate-buffered saline (PBS), pH 7.4. For  $^{99\text{m}}\text{Tc}$  labeling experiments the diabody was further concentrated

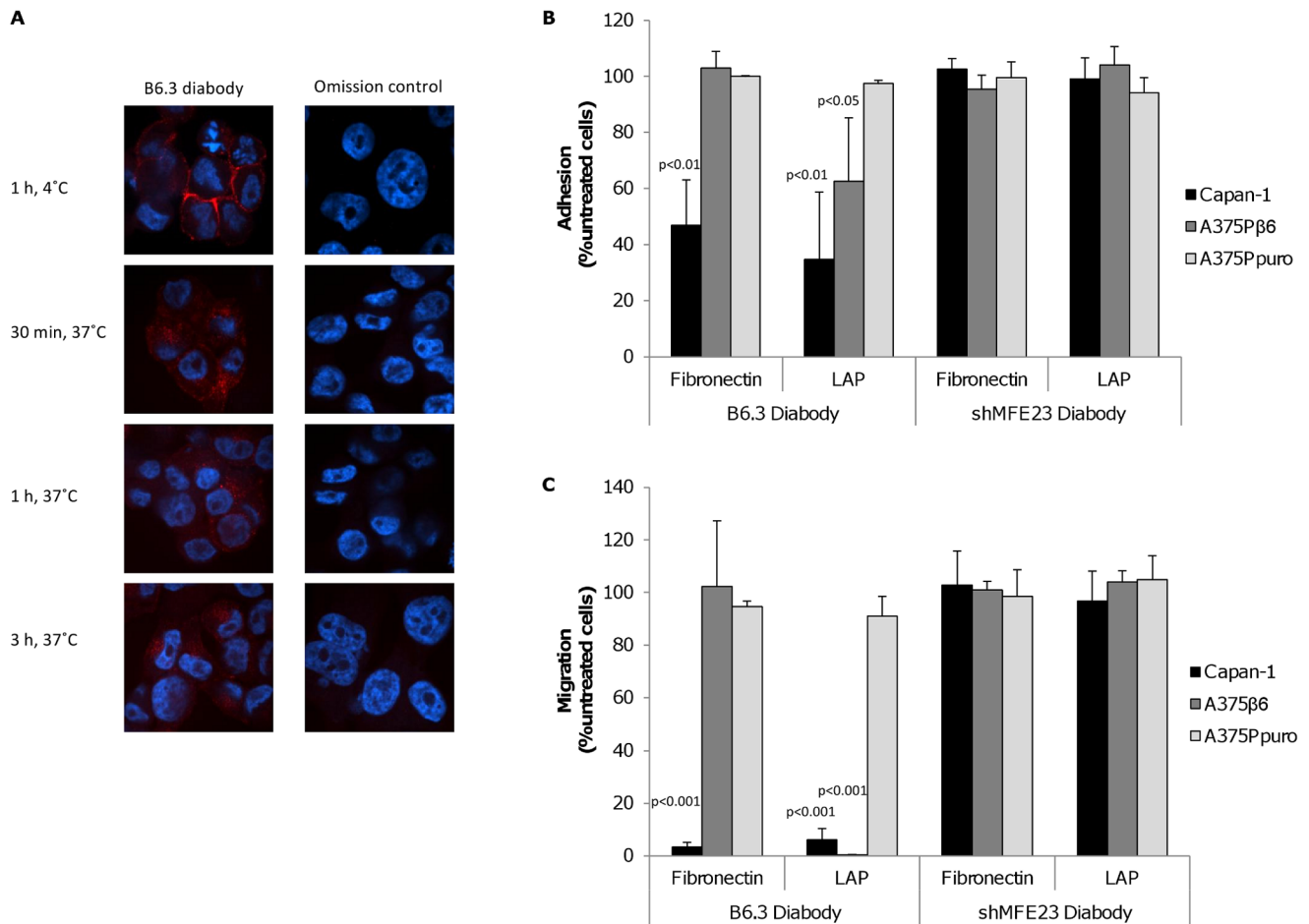


**Figure 2. Treatment of  $\alpha_v\beta_6$ -expressing cells with B6.3 diabody resulted in diabody internalization and blockade of integrin functions.** A) Localization of B6.3 diabody in A375Pβ6 cells by confocal microscopy. B6.3 diabody detection showed membrane pattern of staining at 4°C and internalized when cells were incubated at 37°C for 30 min, 1 h and 3 h. B6.3 diabody was detected using rabbit anti-human IgG followed by Alexa Fluor 546<sup>®</sup>-labeled goat anti-rabbit IgG (red). Cells were also counterstained with Hoechst 33245 (blue). B) Treatment of  $\alpha_v\beta_6$ -expressing cells blocked adhesion to LAP-coated plates (A375Pβ6 and Capan-1 cells) and/or fibronectin-coated plates (Capan-1 cells). Cells were incubated with B6.3 or shMFE23 diabody at 4°C for 1 h and allowed to attach to coated plates for 1 h at 37°C. Treatment with the anti-CEA shMFE23 diabody had no effect on the cell lines used. C) B6.3 diabody treatment inhibited migration towards LAP and fibronectin. As observed in adhesion assays, the diabody inhibited migration of A375Pβ6 cells to LAP and migration of Capan-1 cells to fibronectin and LAP, while targeting CEA had no effect on the cells tested.

doi:10.1371/journal.pone.0073260.g002

to 7.3 mg/ml by application to a 1 ml Ni<sup>2+</sup>-charged HiTrap IMAC SP FF column (GE Healthcare) according to the manufacturer's instructions. Purified protein was analyzed by SDS-PAGE using Tris-glycine gels (16%; Invitrogen) and stained with Coomassie brilliant blue R250 (Sigma). The shMFE23 diabody was produced following the same protocol as for B6.3 diabody production, using the shMFE23 scFv [26] vH and vL domains as template. The purified protein gave a single peak by size exclusion chromatography (data not shown) indistinguishable from that obtained with the B6.3 diabody.

#### Affinity of $\alpha_v\beta_6$ binding to B6.3 diabody by Surface Plasmon Resonance

Affinity of purified B6.3 diabody for  $\alpha_v\beta_6$  was measured by surface plasmon resonance (SPR) using a Biacore T100. The diabody was immobilized on a Research Grade CM5 chip using an amine coupling kit (BIAcore, GE Healthcare). Recombinant  $\alpha_v\beta_6$  protein (R&D Systems) was flown over the immobilized B6.3 diabody in HBS-P buffer (10 mM HEPES, 150 mM NaCl, 0.05%

v/v Surfactant P20, pH 7.4, with addition of 2 mM Ca<sup>2+</sup> and 2 mM Mg<sup>2+</sup> ions) at 30 μL/min at 25°C. Association and dissociation phases occurred over 300 s. Kinetics of binding was calculated from data at 400 nM, 200 nM, 100 nM, 50 nM, 25 nM, 12.5 nM, 6.25 nM and 3.125 nM using the BIAevaluation program. The surface was regenerated with 10 mM Glycine-HCl, pH 2.5. The affinity constant (KD) was obtained by simultaneously fitting the association and dissociation phases of the sensogram from the analyte concentration series using the 1:1 Langmuir model (BIAevaluate software).

#### Flow cytometric analysis of B6.3 diabody binding to $\alpha_v\beta_6$ -expressing cells

A375Pβ6 and A375Ppuro cells were trypsinized, re-suspended in DMEM supplemented with 0.1% (v/v) BSA and 0.1% (w/v) sodium azide (DMEM0.1/0.1) to approximately 5 × 10<sup>6</sup> cells/ml and incubated with various concentrations of B6.3 diabody. Bound diabody was detected with mouse Tetra-His antibody (1 μg/100 μl, Qiagen) and R-PE-conjugated goat anti-mouse IgG

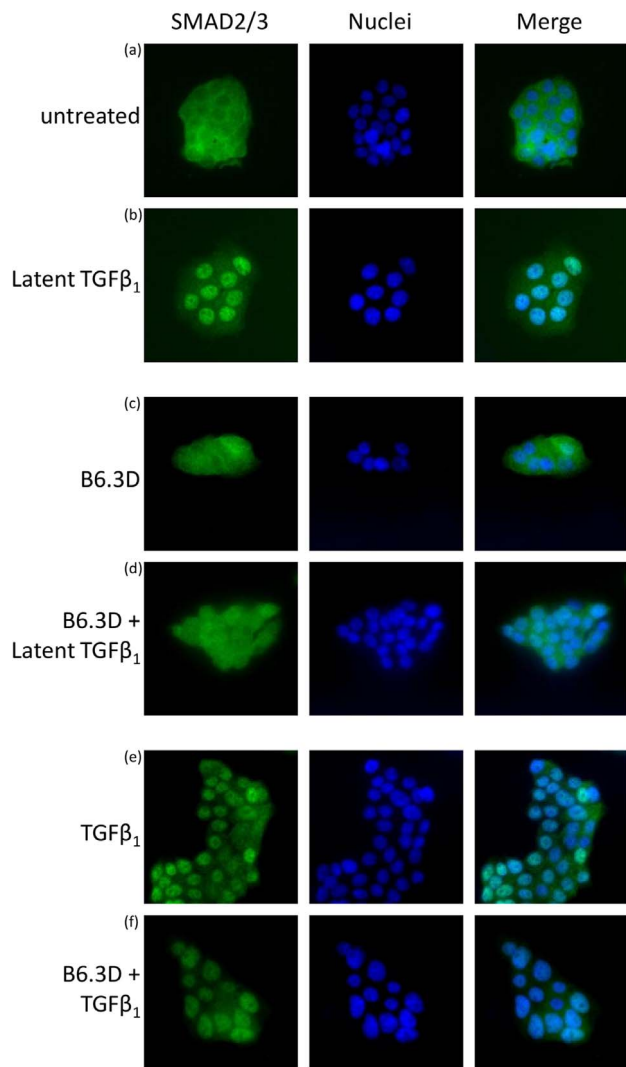


**Figure 3. B6.3 diabody inhibited LAP-mediated Smad2/3 translocation to the nucleus in Capan-1 cells.** Cells were incubated at 4°C in the presence of B6.3 diabody and then treated with LAP or TGF $\beta_1$  (30 min, 37°C); Smad2/3 localization was assessed by confocal microscopy (40X) using rabbit anti-Smad2/3 followed by Alexa Fluor 488<sup>®</sup>-labeled goat anti-rabbit IgG (green); smad2/3 was found in the cytoplasm of starved Capan-1 cells (a) and after treatment with B6.3 diabody (c). Smad2/3 was present in the nuclei in response to treatment with latent TGF $\beta_1$  (b), a translocation that was inhibited by pre-treatment B6.3 diabody (d). TGF $\beta_1$  was used as a positive control (e.f). doi:10.1371/journal.pone.0073260.g003

(BD Pharmingen, 1  $\mu$ g/100 $\mu$ l). Detection antibodies were incubated in DMEM0.1/0.1 for 45 min at 4°C; all incubations were followed by washing with DMEM0.1/0.1. Cells were fixed with IntraStain kit (DakoCytomation, Glostrup, Denmark) and analyzed by flow cytometry using a CyAn ADP High-Performance Flow Cytometer (Becton Dickinson). For binding inhibition studies, A375P $\beta_6$  cells were incubated with mouse anti- $\alpha_v\beta_6$  (10D5, Chemicon International) at various concentrations for 15 min followed by incubation with 100 ng (18.04 nM) of diabody for 30 min. After washing, bound diabody was detected with rabbit anti-hexahistidine IgG (GenScript) at 1  $\mu$ g/100  $\mu$ l, followed by R-PE-conjugated goat anti-rabbit IgG (1  $\mu$ g/100  $\mu$ l, Invitrogen). All incubation and washing steps were in DMEM0.1/0.1 at 4°C. Cells were fixed and analysed as described above.

### <sup>99m</sup>Tc labeling of B6.3 diabody

Sodium [<sup>99m</sup>Tc] pertechnetate was obtained from a <sup>99</sup>Mo/<sup>99m</sup>Tc generator (GE Healthcare, Amersham UK) and converted to [<sup>99m</sup>Tc(CO)<sub>3</sub>(H<sub>2</sub>O)<sub>3</sub>]<sup>+</sup> using an IsoLink<sup>™</sup> kit (generously provided by Covidien, Petten, The Netherlands) according to the manufacturer's instructions. B6.3 diabody was labeled at the C-terminal hexahistidine tag with <sup>99m</sup>Tc by incubating with 750 MBq of [<sup>99m</sup>Tc(CO)<sub>3</sub>(H<sub>2</sub>O)<sub>3</sub>]<sup>+</sup> in a total volume of 574  $\mu$ l at 37°C for 2 h. The labeled protein was separated from the non-incorporated radionuclide by desalting (NAP-10 column, GE Healthcare). Integrity of the radio-labeled protein as a dimer was verified by size-exclusion HPLC on a Biosep-SEC-S 2000 column eluted with 0.1 M phosphate buffer pH 7 at a flow rate of 0.5 ml/min.

### Cell Saturation Binding Assay

The immunoreactivity and affinity of <sup>99m</sup>Tc-labeled B6.3 diabody to  $\alpha_v\beta_6$  was analyzed by a saturation-binding assay using A375P $\beta_6$  cells. Six duplicate test samples containing increasing amounts of <sup>99m</sup>Tc-labeled B6.3 diabody and approximately  $6.5 \times 10^5$  A375P $\beta_6$  cells per experiment were incubated in a total volume of 1 ml of DMEM with 0.1% (v/v) BSA (DMEM0.1) at 4°C for 3 h. Supernatant was removed by centrifugation and cells were washed once with DMEM0.1. An identical series of tubes were prepared in which non-specific binding was determined by addition of 25  $\mu$ g unlabeled diabody to each tube. Non-specific binding was subtracted from total binding to obtain specific binding. Affinity constant (KD) and maximal number of  $\alpha_v\beta_6$  binding sites (Bmax) were determined by non-linear regression analysis using Graphpad prism software.

### Immunofluorescence microscopy of internalization of B6.3 diabody into $\alpha_v\beta_6$ -expressing cells

A375P $\beta_6$  cells were seeded on to glass cover slips at  $2 \times 10^5$  cells/well and incubated for 48 h at 37°C. Cells were then washed with DMEM0.1, incubated with 5  $\mu$ g/ml of B6.3 diabody in 1% BSA/DMEM (DMEM1) for 1 h at 4°C and subsequently washed and incubated in 10% (v/v) FBS/DMEM at 37°C for various time points. After incubation, cells were washed twice with Tris-Cl, pH 7.5, containing 2 mM Ca<sup>2+</sup> and 1 mM Mg<sup>2+</sup> (Tris/M), followed by fixation in 4% paraformaldehyde/Tris/M for 20 min on ice. After washing with PBS, cells were incubated with 10 mM ammonium chloride/PBS for 10 min at room temperature and permeabilized with ice-cold methanol. Finally, cells were blocked with 1% (w/v) BSA/PBS for 30 min at room temperature and stained with 1  $\mu$ g/ml of rabbit anti-human IgG (Jackson Immuno Research, Suffolk, UK) in 1% (w/v) BSA/PBS followed by Alexa Fluor 546<sup>®</sup>-labeled goat anti-rabbit IgG (1:500) (Invitrogen), containing Hoechst trihydrochloride (1:5000) (Invitrogen) in 1% (w/v) BSA/PBS, each for 1 h at 4°C. Cover slips were mounted on slides using ProLong Gold antifade (Invitrogen) and examined using Perkin Elmer Spinning Disc Confocal microscope and Velocity<sup>™</sup> Visualisation Software.

### Adhesion assays

Ninety-six-well plates were coated with 100  $\mu$ l of fibronectin (R&D Systems) at 25  $\mu$ g/ml or LAP (R&D Systems) at 0.5  $\mu$ g/ml for 1 h at 37°C. After coating, plates were washed with PBS and blocked with 1% BSA/PBS at 37°C for 1 h. For blocking experiments, cells were treated with 50  $\mu$ g/ml B6.3 diabody for 1 h at 4°C in DMEM0.1 and seeded at  $5 \times 10^4$  cells/well. After incubation at 37°C for 1 h, plates were extensively washed with PBS to remove non-attached cells and 100  $\mu$ l of a dilution 1:10 of

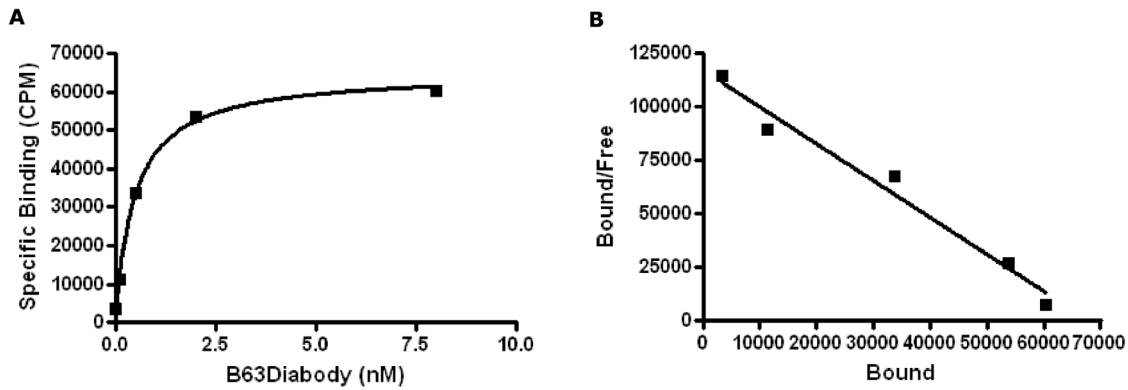


**Figure 4. Labeling with  $^{99m}\text{Tc}$  did not affect B6.3 diabody binding to  $\alpha_v\beta_6$ .** A) Saturation Binding experiment showed concentration-dependent binding of  $^{99m}\text{Tc}$ -labeled diabody to A375P $\beta_6$  cells. Non-specific binding, including 25  $\mu\text{g}$  of unlabeled diabody was subtracted from each data point. KD obtained was  $4.88 \pm 0.32 \times 10^{-8}$  M and BMax was  $2.3 \pm 0.039 \times 10^5$  receptors/cell ( $325 \pm 5.53$  pM/ $8.5 \times 10^5$  cells). B) Scatchard presentation of the data. Each experiment was carried out in duplicate. doi:10.1371/journal.pone.0073260.g004

Prestoblu $^{\text{®}}$  (Invitrogen) was added to each well. Fluorescence signal was measured after incubation at 37°C for 4 h using a Multimode Varioskan plate reader (Thermo Scientific). Results were expressed as percentage of attachment relative to untreated cells with statistical significance analyzed by Student's unpaired t-test.

#### Migration assays

Cell migration was analysed using Transwell assays (Corning, NY, USA) with polycarbonate filters (8  $\mu\text{m}$  pore size). Membrane underside was coated with fibronectin (R&D Systems) at 25  $\mu\text{g}/\text{ml}$  or LAP (R&D Systems) at 0.5  $\mu\text{g}/\text{ml}$  for 1 h at 37°C and blocked with DMEM0.1 for 1 h at 37°C. Cells were treated as described for adhesion assays and seeded in the upper chamber at  $1 \times 10^5$  cells/chamber in 100  $\mu\text{l}$ . The lower chamber was filled with 600  $\mu\text{l}$  DMEM0.1. Plates were then incubated for 20 h at 37°C and cells in the upper chamber were carefully removed using a cotton swap. Migrated cells were fixed with 4% paraformaldehyde, stained with Hoechst trihydrochloride (1:5000) (Invitrogen) for 10 min and counted using a Zeiss AxioImager A1 fluorescence microscope with AxioVision software. Results were expressed as percentage of migrated compared to untreated cells with statistical significance analyzed by Student's unpaired t-test.

#### Immunocytofluorescence for Smad2/3 localization

Capan-1 cells were seeded in cover slips in 10% (v/v) FBS/DMEM and allowed to grow to 70% confluency. Cells were then washed twice in PBS, starved for 24 h in serum-free DMEM and treated with 50  $\mu\text{g}/\text{ml}$  B6.3 diabody for 1 h at 4°C in DMEM0.1. After incubation with the diabody cells were washed twice with PBS and treated with DMEM0.1, latent TGF $\beta_1$  (Cell Signaling Technology) at 50 ng/ml or TGF $\beta_1$  (R&D Systems) at 10 ng/ml for 30 min at 37°C. After extensive washing with PBS, 4% formaldehyde was used to fix the cells (15 min at 4°C). Cells were then permeabilized with 0.3% Triton-X 100 (Sigma) in PBS and cover slips were blocked for 1 h with 5% goat serum before overnight incubation with rabbit anti-Smad2/3 antibody (Cell Signaling Technology) at 4°C. The following day, primary antibody was detected with Alexa Fluor 488 $^{\text{®}}$ -labeled goat anti-rabbit IgG (Invitrogen) containing Hoechst trihydrochloride (Invitrogen). Cover slips were mounted on slides using ProLong Gold antifade (Invitrogen) and examined using a Zeiss AxioImager A1 fluorescence microscope with AxioVision software.

#### In vivo studies

All experiments were conducted with previous approval from the UK Home Office, under PPL 70/6677. Female SCID mice were injected subcutaneously (s.c.) with  $4 \times 10^6$  A375P $\beta_6$  cells in one flank, and  $4 \times 10^6$  A375Ppuro cells in the contralateral flank, in 150  $\mu\text{l}$  serum-free DMEM. Once tumors reached a diameter of around 5 mm, approximately 11  $\mu\text{g}$  (30MBq) per mouse of  $^{99m}\text{Tc}$ -labeled B6.3 diabody in 200  $\mu\text{l}$  PBS was injected intravenously (i.v.). Mice were anaesthetised with isoflurane and imaged 2 h, 5 h and 24 h after injection using a Nano-SPECT/CT scanner (Bioscan, Washington, DC, USA). SPECT images were analysed using *in vivo* Scope software (Bioscan). Mice were sacrificed 24 h after injection of diabody; tissues were excised and radioactivity measured on a gamma counter (LKB Compugamma, Victoria, Australia) alongside standards prepared from the injectate. Uptake of radioactivity in individual tissues was expressed as a percentage of the injected radioactive dose per gram (%ID/g).

## Results

#### Expression and characterisation of B6.3 diabody

B6.3 diabody was generated as soluble protein by fermentation in *P. pastoris* giving a yield of 175 mg/L. The diabody was purified from the bioreactor broth using expanded bed IMAC, exploiting the engineered hexahistidine tag, and concentrated to 2.27 mg/ml. There was no evidence of aggregation when the product was tested by size-exclusion chromatography; diabody eluted as a single peak of >44 kDa, consistent with its calculated MW of 55,322Da (Fig. 1A). The protein was essentially pure as shown by SDS-PAGE and was revealed as a monomer under denaturing conditions (Fig. 1A), consistent with diabody formation by non-covalent association. We next analysed the binding affinity of the purified B6.3 diabody to  $\alpha_v\beta_6$ . SPR showed that  $\alpha_v\beta_6$  bound to B6.3 diabody in a concentration-dependent manner (Fig. 1B) and subsequently remained associated. Fitting of the data to a Langmuir 1:1 model gave an affinity constant (KD) value of  $2.78 \times 10^{-9}$  M and kinetic rate constants of  $k_a = 8.1 \times 10^3 \pm 7.3 \text{ s}^{-1} \text{ M}^{-1}$  and  $k_d = 2.3 \times 10^{-5} \pm 1.4 \times 10^{-7} \text{ s}^{-1}$ .

#### Interactions with $\alpha_v\beta_6$ -expressing cells

Specificity of purified B6.3 diabody for  $\alpha_v\beta_6$  on tumor cells was assessed by flow cytometry using the  $\alpha_v\beta_6$ -expressing cell line, A375P $\beta_6$ , and corresponding  $\alpha_v\beta_6$ -negative A375Ppuro cells. The



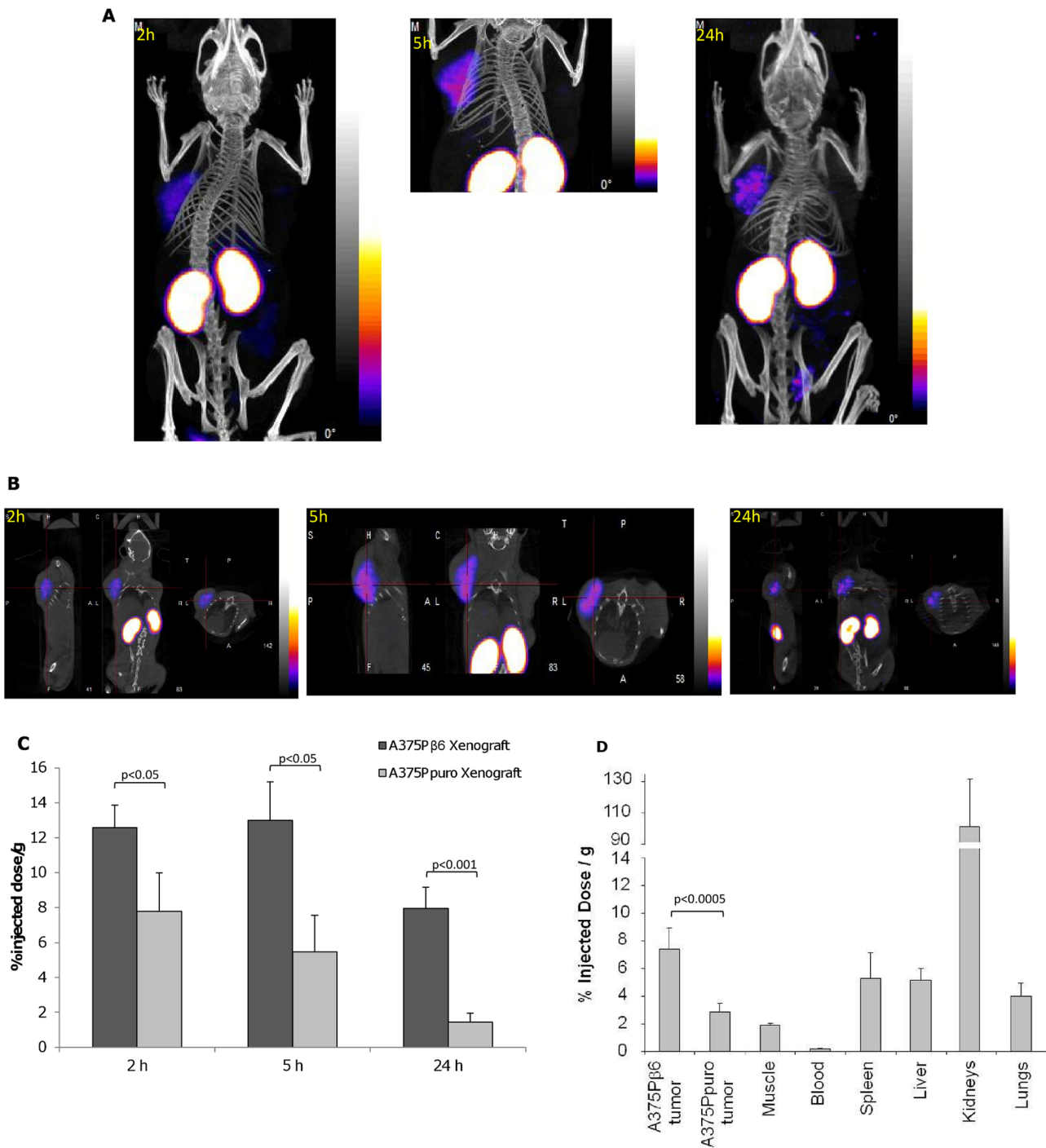


**Figure 5. <sup>99m</sup>Tc-labeled B6.3 diabody localised specifically to  $\alpha_v\beta_6$ -expressing tumors in vivo.** A) A375Pβ6 and A375Ppuro cells were injected subcutaneously on opposite shoulders and <sup>99m</sup>Tc-labeled B6.3 diabody (approximately 11 μg, 30 MBq) was injected intravenously once tumours had developed. Mice were imaged by SPECT/CT as indicated 2 h, 5 h and 24 h after injection. B) SPECT/CT cross sections of the same mice at 2, 5 and 24 h. C) Percent injected doses of <sup>99m</sup>Tc-labeled B6.3 diabody in A375Pβ6 and A375Ppuro tumours from three mice, obtained from these images. D) Biodistribution of <sup>99m</sup>Tc-labeled B6.3 diabody 24 h after injection. Data expressed as % injected dose/g (%ID/g) as mean ± SD for 5 animals. Tumor-to blood ratios at this time point were 40.4 for A375Pβ6 tumours and 15.5 for A375Ppuro tumours. Significance assessed by Student's t-test. doi:10.1371/journal.pone.0073260.g005

results showed that B6.3 diabody bound to the  $\alpha_v\beta_6$ -expressing cells in a concentration-dependent manner (Fig. 1C) but did not bind to the  $\alpha_v\beta_6$ -negative cells when tested at the two highest concentrations (Fig. 1C). The shift in fluorescence intensity

observed for binding to A375Pβ6 cells were similar at 22.6, 45.1 and 90.2 nM, indicating that antigen saturation was reached at these concentrations. To further verify the specificity of the B6.3 diabody to  $\alpha_v\beta_6$ , cells were pre-incubated with an anti- $\alpha_v\beta_6$

antibody, 10D5. This resulted in inhibition of B6.3 diabody binding when 10D5 was used at 10 and 100 nM (Fig. 1D).

Next we tested whether the diabody would internalize specifically into the  $\alpha_v\beta_6$ -expressing cells, as previously reported for other ligand-mimic antibodies targeting this integrin [27]. Cells were treated with B6.3 diabody at 4°C for 1 h to allow binding to the outer cell membrane. Then, temperature was increased to 37°C for different length of time to allow internalization and the resulting cellular distribution of the diabody was revealed after fixation and permeabilization by fluorescence staining. Results of these experiments showed that, upon binding at 4°C, B6.3 diabody was localized at the cell surface (Fig. 2A). When the temperature was raised to 37°C surface staining disappeared and the diabody was found inside the cells after 30 min, 1 h and 3 h of incubation (Fig. 2A).

### B6.3 diabody-mediated blockade of $\alpha_v\beta_6$ biological functions

The  $\alpha_v\beta_6$  integrin is known to have a role in the promotion of cell migration based on interaction with components of the extracellular matrix [6,11,16]. Since the B6.3 diabody contained an RGD motif and internalized as a ligand-mimic antibody, we investigated whether the diabody would exhibit biological effects associated with integrin blockade. First we tested the ability of the diabody to inhibit adhesion and migration of  $\alpha_v\beta_6$ -positive or negative cells to the  $\alpha_v\beta_6$  ligands, LAP and fibronectin. In addition to the stably-transfected A375P $\beta_6$  cells, we included the naturally  $\alpha_v\beta_6$ -expressing pancreatic cancer cell line Capan-1. Treatment with B6.3 diabody at 50  $\mu\text{g}/\text{ml}$  resulted in a reduction in adhesion of A375P $\beta_6$  and Capan-1 cells to LAP-coated plates (Fig. 2B). In addition, we observed a decrease in the number of Capan-1 cells attached to fibronectin-coated plates. The shMFE23 diabody targeting the carcinoembryonic antigen (CEA) was used as control; pre-treatment with this diabody had no effect on the CEA-positive Capan-1 cells or the melanoma cell lines, negative for CEA [17]. The results from Transwell migration assays were more marked as the B6.3 diabody induced an almost complete inhibition of migration towards LAP in both A375P $\beta_6$  and Capan-1 cells (Fig. 2C). In addition, the migration of Capan-1 cells to fibronectin was almost completely inhibited by the diabody, indicating that  $\alpha_v\beta_6$  is the major fibronectin-binding integrin on Capan-1. In contrast, B6.3 diabody did not block A375P $\beta_6$  cells adhering to or migrating on fibronectin (Fig 2C), consistent with our previous data that showed both A375P $\beta_6$  and A375Ppuro express two other fibronectin-binding integrins  $\alpha_5\beta_3$  and  $\alpha_5\beta_1$  [17]. No effect on adhesion or migration was observed in the  $\alpha_v\beta_6$ -negative cell line A375Ppuro or after addition of an irrelevant diabody, indicating that the B6.3-dependent inhibition was  $\alpha_v\beta_6$ -specific.

The  $\alpha_v\beta_6$  integrin is known to activate TGF $\beta_1$  upon interaction with its latent form (LAP-TGF $\beta_1$  complex), resulting in TGF $\beta$ -induced smad2/3 phosphorylation and subsequent translocation of smad2/3 to the nucleus [7]. We hypothesized that binding of B6.3 diabody to  $\alpha_v\beta_6$  would inhibit its interaction with latent TGF $\beta_1$  and downstream Smad2/3 translocation. We showed that smad2/3 localized in the cytoplasm in serum-starved Capan-1 cells (Fig. 3(a)). Incubation with B6.3 diabody had no effect on smad2/3 localization (Fig. 3(c)), while treatment with latent TGF $\beta_1$  resulted in nuclear translocation of Smad2/3 (Fig. 3(b)). We next tested the localization of smad2/3 after incubation with the B6.3 diabody. Our data showed that B6.3 diabody inhibited Smad2/3 nuclear translocation mediated by latent TGF $\beta_1$  (Fig. 3(d)), indicating that the diabody blocked smad2/3 activation. Active TGF $\beta_1$  showed Smad2/3 translocation in B6.3-treated cells

(Fig. 3(f)), since the active form does not require prior integrin interactions.

### Labeling efficiency of B6.3 diabody

In order to determine the efficacy of the diabody for  $\alpha_v\beta_6$  targeting *in vivo*, B6.3 diabody was labeled with  $^{99\text{m}}\text{Tc}$ . This radionuclide was chosen as it has been described previously to be appropriate for use with internalizing antibody fragments [28] and the chemistry for conjugation to the hexahistidine tag is commercially available using the IsoLink<sup>™</sup> kit. After labelling, the resulting  $^{99\text{m}}\text{Tc}$ -labeled diabody had a specific activity of 2.7MBq/ $\mu\text{g}$  and remained a dimer when tested by size-exclusion chromatography (data not shown). Strength and specificity of interaction of  $^{99\text{m}}\text{Tc}$ -labeled diabody with purified  $\alpha_v\beta_6$  protein was evaluated using a saturation binding experiment which revealed a concentration-dependent increase of  $^{99\text{m}}\text{Tc}$ -B6.3 diabody (Fig. 4A). The specificity of interaction was tested by inhibition of binding by unlabeled diabody. The non-specific binding obtained from the inhibition experiments was subtracted from the total radioactivity to obtain specific binding. When tested on cells, the affinity constant derived from non-linear regression analysis of  $^{99\text{m}}\text{Tc}$ -labeled B6.3 diabody was found to be in the nanomolar range, at  $4.88 \pm 0.32 \times 10^{-8}$  M. The maximal number of  $\alpha_v\beta_6$  binding sites (Bmax) was derived to be  $2.3 \pm 0.039 \times 10^5$  per cell. The Scatchard analysis, which showed a linear correlation (Fig. 4B), was in agreement with a single affinity binding site for the interaction.

### Targeting of B6.3 diabody to $\alpha_v\beta_6$ -expressing tumors *in vivo*

To determine the specificity of the B6.3 diabody *in vivo*,  $^{99\text{m}}\text{Tc}$ -labeled diabody was administered to SCID mice bearing flanking tumors of A375P $\beta_6$  and A375Ppuro cells. Localization of labeled diabody was monitored by whole body cross-section imaging using NanoSPECT/CT. Results of these experiments showed that the  $\alpha_v\beta_6$ -expressing A375P $\beta_6$  tumor was detected with the radio-labeled diabody 2h after injection and remained detectable after 5 h and 24 h (Fig. 5A, 5B). Quantification revealed significantly more radioactivity in the  $\alpha_v\beta_6$ -expressing tumors when compared to the A375Ppuro tumors at all three time points; the uptake was highest 5 h after injection and considerably reduced after 24 h but remained still clearly detectable (Fig. 5C). The highest normal tissue activity was found in the kidneys, a typical pattern found for radio-metal-labeled compounds due to the excretion of  $^{99\text{m}}\text{Tc}$ -labeled compound by this organ.

Twenty-four hours after injection and imaging, the mice were sacrificed and biodistribution of  $^{99\text{m}}\text{Tc}$ -labeled diabody was determined (Fig. 5D). The data showed that %ID/g obtained in A375P $\beta_6$  tumors was significantly higher ( $p < 0.0005$ ) than that in the A375Ppuro tumors, in agreement with quantification from imaging at this time point. Tumor-to-Blood ratios of 40 were obtained for the  $\alpha_v\beta_6$  positive tumor whereas the  $\alpha_v\beta_6$  negative tumor gave a ratio of 15.5. The kidney had the highest %ID/g of any organ in agreement with the imaging results. Imaging and biodistribution studies showed that  $^{99\text{m}}\text{Tc}$ -labeled diabody targets specifically to  $\alpha_v\beta_6$ -expressing tumors *in vivo* and is detectable 24 h after injection with tumor-to-blood ratios suitable for imaging.

### Discussion

This work describes the generation and characterization of a novel diabody that specifically targets the  $\alpha_v\beta_6$  integrin. The diabody was produced as a soluble secreted protein in *P. pastoris*, allowing rapid production using a process readily adaptable to

manufacture of clinical grade material [24,25]. The engineered hexahistidine tag allowed purification and successful labeling with  $^{99m}\text{Tc}$ , without affecting the nanomolar binding affinity of the diabody on cells *in vitro*.

Our studies also showed that the diabody inhibited adhesion and migration of the  $\alpha_v\beta_6$ -transfected melanoma cell line, A375P $\beta_6$  and the pancreatic adenocarcinoma cell line, Capan-1, to LAP. This is the desired function-blocking activity of anti- $\alpha_v\beta_6$  and has been observed with whole anti- $\alpha_v\beta_6$  antibodies that block *in vitro* migration of  $\alpha_v\beta_6$ -positive Detroit 562 human pharyngeal carcinoma cells and inhibit tumor growth *in vivo* by suppressing TGF $\beta$  activation [16,27]. When interactions via fibronectin, a less specific ligand, were investigated, the diabody was found to inhibit adhesion and migration of Capan-1 cells but not A375P $\beta_6$  cells. This highlights the specificity of B6.3 because A375P $\beta_6$  cells express other fibronectin-binding integrins [17] that would not be blocked by an  $\alpha_v\beta_6$ -specific agent. The  $\alpha_v\beta_6$  integrin activates latent-TGF $\beta$  first by binding to LAP and then through cortical actin-dependent mechanical forces that causes distortion of the LAP molecule, releasing the TGF $\beta$  [29,30]. Targeting  $\alpha_v\beta_6$  with the B6.3 diabody inhibited this interaction with LAP, resulting in inhibition of Smad2/3 translocation to the nucleus.

The role of  $\alpha_v\beta_6$ -dependent TGF $\beta$  activation in cancer has been investigated in a number of studies [31,32,33,34,35], that illustrate both the potential and complexity associated with this target. For example, when  $\alpha_v\beta_6$  was blocked with antibodies in the early stages of disease in a transgenic pancreatic cancer mouse model, this accelerated cancer progression when SMAD4 was functional, but not in SMAD4-null animals [34]. In separate studies  $\alpha_v\beta_6$  promoted cancer growth and liver metastasis through activation of TGF $\beta$  [11,36]. Thus, the functional blockade of  $\alpha_v\beta_6$  has positive therapeutic implications due to the potential inhibition of TGF $\beta$ , although TGF $\beta$  can also act as a tumour suppressor in normal epithelium and pre-malignant transformed epithelial cells. However, cancer cells often develop mutations that prevent TGF $\beta$ -mediated growth inhibition, making TGF $\beta$  a strong tumor promoter [32,33]. Therefore therapeutic antibody blockade of  $\alpha_v\beta_6$  can suppress tumour growth [16,35] but the molecular phenotype of the tumor must be taken into consideration.

When tested for  $\alpha_v\beta_6$  localization *in vivo*, the radiolabeled diabody showed specific targeting of  $\alpha_v\beta_6$ -positive tumours, detectable as early as two hours after injection. Signal was measurable over 24 hours, although intensity was highest five hours after injection. Radiolabeling with  $^{99m}\text{Tc}$ , using site-specific attachment to the engineered hexahistidine tag, was found to be simple and efficient. Furthermore, use of  $^{99m}\text{Tc}$  allowed residualization of the signal within the tumor upon internalization of the diabody. These characteristics, combined with the ease of production of B6.3 and its favourable biodistribution *in vivo*, make this diabody an attractive tool for clinical imaging.

## References

- Patsenker E, Wilkens L, Banz V, Osterreicher CH, Weimann R, et al. (2010) The alphavbeta6 integrin is a highly specific immunohistochemical marker for cholangiocarcinoma. *J Hepatol* 52: 362–369.
- Bandyopadhyay A, Raghavan S (2009) Defining the role of integrin alphavbeta6 in cancer. *Curr Drug Targets* 10: 645–652.
- Sipos B, Hahn D, Carceller A, Piulats J, Hedderich J, et al. (2004) Immunohistochemical screening for beta6-integrin subunit expression in adenocarcinomas using a novel monoclonal antibody reveals strong up-regulation in pancreatic ductal adenocarcinomas *in vivo* and *in vitro*. *Histopathology* 45: 226–236.
- Bates RC (2005) Colorectal cancer progression: integrin alphavbeta6 and the epithelial-mesenchymal transition (EMT). *Cell Cycle* 4: 1350–1352.
- Hazelbag S, Kenter GG, Gorter A, Dreef EJ, Koopman LA, et al. (2007) Overexpression of the alpha v beta 6 integrin in cervical squamous cell carcinoma is a prognostic factor for decreased survival. *J Pathol* 212: 316–324.
- Thomas GJ, Nystrom ML, Marshall JF (2006) Alphavbeta6 integrin in wound healing and cancer of the oral cavity. *J Oral Pathol Med* 35: 1–10.
- Shi M, Zhu J, Wang R, Chen X, Mi L, et al. (2011) Latent TGF-beta structure and activation. *Nature* 474: 343–349.
- Thomas GJ, Lewis MP, Hart IR, Marshall JF, Speight PM (2001) AlphaVbeta6 integrin promotes invasion of squamous carcinoma cells through up-regulation of matrix metalloproteinase-9. *Int J Cancer* 92: 641–650.
- Munger JS, Huang X, Kawakatsu H, Griffiths MJ, Dalton SL, et al. (1999) The integrin alpha v beta 6 binds and activates latent TGF beta 1: a mechanism for regulating pulmonary inflammation and fibrosis. *Cell* 96: 319–328.
- Zhang ZY, Xu KS, Wang JS, Yang GY, Wang W, et al. (2008) Integrin alphavbeta6 acts as a prognostic indicator in gastric carcinoma. *Clin Oncol (R Coll Radiol)* 20: 61–66.

The diabody format has not yet been fully exploited as a cancer targeting agent, but it has many attractive features. The bivalency of diabodies conferred by their dimeric structure holds the advantage of higher tumor uptake compared to scFv fragments, resulting in higher signals when used as imaging agents [37]. Also the bigger size of diabodies in relation to scFv increases their circulatory half life, resulting in higher accumulation in the tumor, while achieving better contrast at short time points than bigger engineered fragments such as minibodies [38]. However, despite higher contrast and early imaging, radiometal-labeling of diabodies also results in considerable kidney retention, as shown in our current study and by other groups [22,37,38]. This can be problematic if imaging is desirable in close areas. Attachment of polyethylene glycol (PEG) to diabodies has shown to significantly lower kidney retention [22] and improvement of pharmacokinetics [21], resulting in increased circulating time that did not affect the collection of optimal images within 24 hours. The increased circulating time could in fact be advantageous if diabodies are to be used for therapeutic purposes, which required maximum tumor accumulation. In this sense, the internalization of the B6.3 could be clinically useful for delivery of toxic compounds such as the radioisotope, conjugated toxic agents should or small toxic drugs, such as pyrrolbenzodiazepines (PBDs), that are active within target cells.

In summary, the B6.3 diabody described in our study bound specifically to  $\alpha_v\beta_6$  *in vitro* and targeted specifically to  $\alpha_v\beta_6$ -expressing tumors *in vivo*. In addition, the diabody retained the biological properties of ligand-mimicking antibodies; it showed internalization upon binding to  $\alpha_v\beta_6$ , successfully blocked  $\alpha_v\beta_6$ -dependent adhesion and migration to LAP and fibronectin and inhibited smad2/3 nuclear translocation upon treatment with latent TGF $\beta_1$ . Based on its function-blocking activity and specific targeting to  $\alpha_v\beta_6$ -positive cells *in vivo*, the B6.3 diabody has potential as an imaging agent or a building block for generation of therapeutics by chemical coupling of small cytotoxic molecules or addition of toxic agents.

## Acknowledgments

The authors thank Hector Knight (Covidien) for providing the Isolink kits. We are also grateful to Professor Ian Hart for his valuable intellectual suggestions in this study.

## Author Contributions

Conceived and designed the experiments: HK EM GJT TM JFM SJM KC. Performed the experiments: HK EM JB DE BT JF CP. Analyzed the data: HK EM JB DE BT CP GJT SJM KC. Contributed reagents/materials/analysis tools: HK EM BT GJT JFM SJM KC. Wrote the paper: HK EM KC. Critical review of manuscript: HK EM BT GJT TM JFM SJM KC.



11. Yang GY, Xu KS, Pan ZQ, Zhang ZY, Mi YT, et al. (2008) Integrin alpha v beta 6 mediates the potential for colon cancer cells to colonize in and metastasize to the liver. *Cancer Sci* 99: 879–887.
12. Mamuya FA, Duncan MK (2012)  $\alpha_v$  integrins and TGF- $\beta$ -induced EMT: a circle of regulation. *J Cell Mol Med* 16: 445–455.
13. Bates RC, Mercurio AM (2005) The epithelial-mesenchymal transition (EMT) and colorectal cancer progression. *Cancer Biol Ther* 4: 365–370.
14. Singh A, Greninger P, Rhodes D, Koopman L, Violette S, et al. (2009) A gene expression signature associated with “K-Ras addiction” reveals regulators of EMT and tumor cell survival. *Cancer Cell* 15: 489–500.
15. Yang SB, Du Y, Wu BY, Xu SP, Wen JB, et al. (2012) Integrin  $\alpha_v\beta_6$  promotes tumor tolerance in colorectal cancer. *Cancer Immunol Immunother* 61: 335–342.
16. Van Aarsen LA, Leone DR, Ho S, Dolinski BM, McCoon PE, et al. (2008) Antibody-mediated blockade of integrin alpha v beta 6 inhibits tumor progression in vivo by a transforming growth factor- $\beta$ -regulated mechanism. *Cancer Res* 68: 561–570.
17. Kogelberg H, Tolner B, Thomas GJ, Di Cara D, Minogue S, et al. (2008) Engineering a single-chain Fv antibody to alpha v beta 6 integrin using the specificity-determining loop of a foot-and-mouth disease virus. *J Mol Biol* 382: 385–401.
18. Holliger P, Prospero T, Winter G (1993) “Diabodies”: small bivalent and bispecific antibody fragments. *Proc Natl Acad Sci U S A* 90: 6444–6448.
19. Wu AM, Yazaki PJ (2000) Designer genes: recombinant antibody fragments for biological imaging. *Q J Nucl Med* 44: 268–283.
20. Adams GP, Schier R, McCall AM, Crawford RS, Wolf EJ, et al. (1998) Prolonged in vivo tumour retention of a human diabody targeting the extracellular domain of human HER2/neu. *Br J Cancer* 77: 1405–1412.
21. Holliger P, Hudson PJ (2005) Engineered antibody fragments and the rise of single domains. *Nat Biotechnol* 23: 1126–1136.
22. Li L, Turatti F, Crow D, Bading JR, Anderson AL, et al. (2010) Monodispersed DOTA-PEG-conjugated anti-TAG-72 diabody has low kidney uptake and high tumor-to-blood ratios resulting in improved  $^{64}\text{Cu}$  PET. *J Nucl Med* 51: 1139–1146.
23. DiCara D, Rapisarda C, Sutcliffe JL, Violette SM, Weinreb PH, et al. (2007) Structure-function analysis of Arg-Gly-Asp helix motifs in alpha v beta 6 integrin ligands. *J Biol Chem* 282: 9657–9665.
24. Tolner B, Smith L, Begent RH, Chester KA (2006) Expanded-bed adsorption immobilized-metal affinity chromatography. *Nat Protoc* 1: 1213–1222.
25. Tolner B, Smith L, Begent RH, Chester KA (2006) Production of recombinant protein in *Pichia pastoris* by fermentation. *Nat Protoc* 1: 1006–1021.
26. Graff CP, Chester K, Begent R, Wittrop KD (2004) Directed evolution of an anti-carcinoembryonic antigen scFv with a 4-day monovalent dissociation half-time at 37 degrees C. *Protein Eng Des Sel* 17: 293–304.
27. Weinreb PH, Simon KJ, Rayhorn P, Yang WJ, Leone DR, et al. (2004) Function-blocking integrin  $\alpha_v\beta_6$  monoclonal antibodies: distinct ligand-mimetic and nonligand-mimetic classes. *J Biol Chem* 279: 17875–17887.
28. He J, Wang Y, Feng J, Zhu X, Lan X, et al. (2010) Targeting prostate cancer cells in vivo using a rapidly internalizing novel human single-chain antibody fragment. *J Nucl Med* 51: 427–432.
29. Giacomini MM, Travis MA, Kudo M, Sheppard D (2012) Epithelial cells utilize cortical actin/myosin to activate latent TGF- $\beta$  through integrin  $\alpha_v(\beta_6)$ -dependent physical force. *Exp Cell Res* 318: 716–722.
30. Sheppard D (2003) Functions of pulmonary epithelial integrins: from development to disease. *Physiol Rev* 83: 673–686.
31. Roberts AB, Wakefield LM (2003) The two faces of transforming growth factor beta in carcinogenesis. *Proc Natl Acad Sci U S A* 100: 8621–8623.
32. Meulmeester E, Ten Dijke P (2011) The dynamic roles of TGF- $\beta$  in cancer. *J Pathol* 223: 205–218.
33. Elliott RL, Blobe GC (2005) Role of transforming growth factor Beta in human cancer. *J Clin Oncol* 23: 2078–2093.
34. Hezel AF, Deshpande V, Zimmerman SM, Contino G, Alagesan B, et al. (2012) TGF- $\beta$  and  $\alpha_v\beta_6$  integrin act in a common pathway to suppress pancreatic cancer progression. *Cancer Res* 72: 4840–4845.
35. Eberlein C, Kendrew J, McDaid K, Alfred A, Kang JS, et al. (2012) A human monoclonal antibody 264RAD targeting  $\alpha_v\beta_6$  integrin reduces tumour growth and metastasis, and modulates key biomarkers in vivo. *Oncogene*.
36. Lee MS, Kim TY, Kim YB, Lee SY, Ko SG, et al. (2005) The signaling network of transforming growth factor beta1, protein kinase Cdelta, and integrin underlies the spreading and invasiveness of gastric carcinoma cells. *Mol Cell Biol* 25: 6921–6936.
37. Wu AM, Olafsen T (2008) Antibodies for molecular imaging of cancer. *Cancer J* 14: 191–197.
38. Sundaresan G, Yazaki PJ, Shively JE, Finn RD, Larson SM, et al. (2003) 124I-labeled engineered anti-CEA minibodies and diabodies allow high-contrast, antigen-specific small-animal PET imaging of xenografts in athymic mice. *J Nucl Med* 44: 1962–1969.